Analytica Chimica Acta 1116 (2020) 62–69

Contents lists available at ScienceDirect

Analytica Chimica Acta

journal homepage: www.elsevier.com/locate/aca

Ultrasensitive detection of microRNA based on a homogeneous label-free electrochemical platform using G-triplex/methylene blue as a signal generator

Ling-Li Zhao , Hui-Yu Pan , Xin-Xiang Zhang , Ying-Lin Zhou *

Beijing National Laboratory for Molecular Sciences (BNLMS), MOE Key Laboratory of Bioorganic Chemistry and Molecular Engineering, College of Chemistry and Molecular Engineering, Peking University, Beijing, 100871, China

HIGHLIGHTS

- A homogeneous electrochemical biosensor for miRNA detection has been fabricated with G-triplex DNA/methylene blue.
- An efficient two-stage amplification system was employed to improve the detection performances.
- A detection limit of 0.45 fM with single-base recognition can be realized.
- Target microRNA in cancer cell-derived RNA samples was directly quantified.

GRAPHICAL ABSTRACT

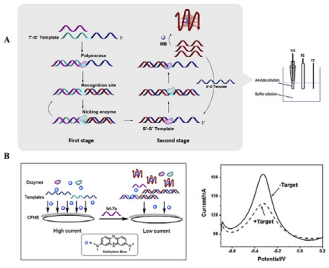

The strategy of G3-EXPAR for miRNA detection

ARTICLE INFO

Article history:
Received 5 April 2020
Received in revised form
11 April 2020
Accepted 14 April 2020
Available online 15 April 2020

Keywords:
G-triplex DNA
MicroRNA
Isothermal exponential amplification
Label-free
Homogeneous electrochemical biosensor

ABSTRACT

The electrochemical methods for microRNA (miRNA) detection have received increasing attention because high portability and affordability of electrochemical biosensors may facilitate point-of-care quantitative detection of miRNAs. Among these biosensors, the homogenous label-free electrochemical biosensors for miRNAs are rarely reported due to the lack of a universal and efficient signal read-out-mode. A newly discovered G-triplex, 5′-CTGGGAGGGAGGGA-3' (denoted as G3), can specifically bind with methylene blue (MB), leading to a significant decrease of the diffusion current of MB. By using miRNAs as a driving force, a two-stage isothermal exponential amplification reaction was proposed to generate G3 through miRNAs. The generated G3 can combine with MB and produce observable current changes, which depend on the concentration of miRNAs. Therefore, a novel homogeneous label-free electrochemical biosensor for miRNA detection was successfully constructed. By choosing let-7a, the down-regulation of which is possibly associated with the over-expression of RAS and HMGA2 oncogenes, as a model, we discovered that this biosensor demonstrated excellent analytical performance in detecting let-7a, with an ultralow limit of detection (0.45 fM) and high specificity (discriminating one nucleotide variation). Moreover, the proposed biosensor was successfully applied in monitoring the expression levels of the low-abundant miRNAs in the human lung adenocarcinoma cell lines. This assay successfully verified the feasibility of G-triplex/MB as an efficient and sensitive probe for immobilization-free and label-free electrochemical detection of nucleic acids, which would greatly promote the rapid development of homogeneous label-free electrochemical biosensors.

* Corresponding author.
E-mail address: zhouyl@pku.edu.cn (Y.-L. Zhou).

https://doi.org/10.1016/j.aca.2020.04.037
0003-2670/

1. Introduction

MicroRNAs (miRNAs), a class of short (19–24 bases) non-coding RNAs, are endogenous in many animal and plant genomes, which have been recognized to be one of the major regulatory gene families in eukaryotic cells recently. To date, over 1000 human miRNAs have been identified, which can target more than 30% of the human genome [1]. Apart from being post-transcriptional regulators, increasing evidence has suggested that abnormal expression of certain miRNAs is closely related to a variety of diseases and disorders, especially cancers [2]. The close correlation between dysregulation of miRNA expression and human cancers has intrigued intense interests to explore the possibility of using miRNAs to classify human cancers, and for utilization as cancer-specific biomarkers for clinical diagnostics and research [3]. Hence, effective detection and quantitation of miRNAs are of great significance for biomedical research, early clinical diagnosis, the pathogenesis of diseases, and therapeutic intervention [4].

Although northern-blotting analysis has been well established as the standard method for detecting miRNAs [5], the microarray approach is becoming increasingly popular because of their high-throughput-screening capability [6]. Nevertheless, these detection methods are not satisfactory in terms of sensitivity and specificity because miRNAs are not only tiny and rare but also tend to share similar sequences [7]. To improve the sensitivity and specificity of the approaches for miRNA analysis, real-time PCR has been developed to be one of the most sensitive and practical methods [8]. However, the short length of miRNAs makes the PCR design very sophisticated. Stem-loop DNA probes, locked nucleic acid (LNA)-modified DNA probes, or doubly fluorescence-labeled TaqMan probes are usually used to improve PCR-based assays, and these probes greatly increase the experimental cost and the complexity of the technical requirement. In terms of the limitations of the traditional methods, various amplification methods including rolling circle amplification [9], hybridization chain reaction [10], catalytic hairpin assembly [11], etc. are designed to develop efficient and simple methods for miRNA detection combined with different detection technologies such as colorimetry [7], fluorescence [12], capillary electrophoresis [13], and electrochemistry [14,15]. Among them, electrochemical assays for miRNA detection have received increasing attention because the electrochemical platform with high portability and affordability could be a powerful tool for miRNA detection at the point of care [16–18].

Most electrochemical methods for miRNAs detection are based on heterogeneous format [18–20] where the immobilization of DNA probes on the electrode surface is necessary. Despite the high sensitivity, the labeling process is laborious or expensive. Novel strategies such as probe electrodeposition onto electrode [21] and the use of non-DNA-based neutravidin probes [22,23] have been reported to methodologically optimize the immobilization process. However, homogenous electrochemical biosensors have the advantages of simplicity, rapidity, low cost and reliability, which could solve the tricky problems on heterogeneous ones. To date, the studies on the strategies for immobilization-free electrochemical miRNA sensors mainly use target-triggered electroactive molecules release (e.g., $[Ru(NH_3)_6]^{3+}$ [24], methylene blue (MB) [25], $[Fe(CN)_6]^{3+}$ [26], and tetramethylbenzidine [25]) and redox recycling as the signal indicators. Nevertheless, those electrochemical methods generally require the complex synthesis of nanoparticles or metal–organic frameworks to entrap the electroactive molecules. Thus, a universal, simple, sensitive and efficient signal read-out-mode for homogenous electrochemical sensors is strongly demanded.

Recently, we reported MB was an excellent intercalating probe of a G-triplex DNA with a sequence of 5′-CTGGGAGGGAGGGA-3’ (denoted as G3), which was a kind of uncanonical nucleic acids. Due to the highly selective discrimination when binding G3 over dsDNA and ssDNA, MB has served as a reporter of label-free homogeneous electrochemical aptasensor [27]. To meet the demand for sensitively detecting the trace amounts of miRNA in the real sample, there still exist two challenges: a) how to convert target miRNA into G3 proportionally, and b) how to amplify the trace amounts of G3 effectively to provide enough sensitivity for signal read-out. Isothermal exponential amplification reaction (EXPAR) was introduced, which displayed high amplification efficiency (10^6–10^8) for short oligonucleotides in a short time (<30 min) and was very suitable to amplify trace amounts of a specific sequence to micromolar levels [28–30]. Therefore, a label-free, homogeneous strategy based on EXPAR using G3/MB complex as a signal generator (denoted as G3-EXPAR) was proposed for ultrasensitive detection of miRNA. The addition of target miRNA initiated the two-stage EXPAR reactions, which contained the conversion of miRNA into G3 in the first stage and the exponential amplification of G3 in the second stage. The enormous amounts of G3 were released and specifically bound with MB, causing obvious current changes of MB for the detection of the low level of miRNA in a simple manner.

2. Experimental sections

2.1. Materials and reagents

RNA and DNA sequences were synthesized from Sangon Biotech. Co., Ltd. (Shanghai, China) and their sequences were shown in Table S1. The Vent (exo-) DNA polymerase and nicking endonuclease Nt. BstNBI were purchased from New England Biolabs (Beverly, MA). Deoxynucleotide mixture (dNTPs) was bought from Takara Biotechnology Co. Ltd (Dalian, China). SYBR-Green I (20X) in dimethyl sulphoxide (DMSO) was obtained from Xiamen Zeesan Biotechnology (Xiamen, China). MB was purchased from Beijing Chemical Reagent Co. (Beijing, China). A 100 mM stock solution (in DMSO) was stored at −20 °C. Ammonium acetate (NH_4Ac) was purchased from Sigma-Aldrich (St Louis, MO). Acetonitrile (ACN) was purchased from J. T. Baker. KCl was from Beijing Chemical Reagent Co. (Beijing, China). All reagents involved RNA experiments were prepared in RNase-free Water purchased from Takara (Beijing, China).

2.2. G3-EXPAR for miRNA assay

The first stage of G3-EXPAR was performed at a volume of 10 μL containing T′-G′ template (200 nM), dNTPs (375 μM), Nt. BstNBI (0.4 U/μL), Vent (exo-) DNA polymerase (0.05 U/μL), different concentrations of miRNA let-7a, 1X ThermoPol buffer and 0.5X Nt. BstNBI buffer. The mixture was incubated at 55 °C for 60 min and stored at 4 °C. Then, 1 μL of the reaction sample was taken out for the second stage of EXPAR. The second-stage reaction was prepared separately as part A and part B solutions. Part A consisted of G′-G′ template, 1 μL of solution from the first stage reaction, Nt. BstNBI buffer and dNTPs. Part B consisted of the nicking endonuclease Nt. BstNBI, Vent (exo-) DNA polymerase and ThermoPol buffer. Part A and Part B were mixed immediately containing G′-G′ template (100 nM), 1 μL of solution from first-stage reaction, Nt. BstNBI (0.4 U/μL), Vent (exo-) DNA polymerase (0.05 U/μL), dNTPs (375 μM), 1 X ThermoPol buffer (20 mM Tris-HCl, pH 8.8, 10 mM KCl, 10 mM $(NH_4)_2SO_4$, 2 mM $MgCl_2$, 0.1% Triton X-100) and 0.5 X Nt. BstNBI buffer (25 mM Tris-HCl, pH 7.9, 50 mM NaCl, 5 mM $MgCl_2$, 0.5 mM DTT). The mixture at a volume of 10 μL was incubated at 55 °C for 15 min and quenched at 4 °C. The total amplification time was about 75 min. The product was kept at 4 °C for subsequent electrochemical analysis.

2.3. Electrochemical measurements

A CHI 660C electrochemical workstation (Shanghai Chenhua Instruments Co., Shanghai, China) was employed to undertake the electrochemical experiments. All measurements were carried out in the miniaturized electrochemical device designed in our previous work [31]. The cylindrical carbon fiber microelectrode (CFME) which diameter was about 7 μm as a working electrode was inserted into the micropipette tip containing 20 μL of the analyte solution. The micropipette tip was then placed in a homemade glass cell containing Tris-HCl buffer. An Ag/AgCl reference electrode and a Pt counter electrode were used to form a full three-electrode system. Square wave voltammetry (SWV) was recorded at a frequency of 200 Hz, pulse amplitude of 25 mV, and with an incremental potential of 4 mV over a potential range of −0.7 to 0.2 V. 24 μL solution from amplification reaction was mixed with 1.5 μL 10 μM MB, 3 μL 500 mM KCl, and 1.5 μL water (All prepared in Tris-HCl buffer, pH 7.4), where KCl was generally used to stabilize the G-triplex structure. A 20 μL of the analyte solution indrawing in micropipette tip was used for performing the electrochemical measurement via the above electrochemical device.

2.4. Liquid chromatography electrospray ionization tandem mass spectrometry (LC-ESI-MS) measurement

The LC-ESI-MS quantification of produced G3 in the amplification reaction was performed on the LC-ESI-MS system consisting of a Thermo Q-Exactive Mass Spectrometer (Thermo, USA) with an ESI source (Turbo Ionspray) and a Thermo Scientific Dionex Ultimate 3000 HPLC (Thermo, USA). Data acquisition and processing were performed using Xcalibur Software (Thermo, USA). The HPLC separation was performed on a Zorbax Stablebond Analytical SB-C18 column (2.1 mm × 100 mm, 3.5 μm, Agilent Technologies, USA) at 20 °C. 20 mM NH_4Ac (pH 9, solvent A) and ACN (solvent B) were employed as the mobile phases. A gradient of 30–100% B for 4 min and 100% B for 5 min was used. The flow rate of the mobile phase was set at 0.3 mL min^{-1}. The mass spectrometry detection was performed under negative ESI mode. Data were acquired over the MS scan range of 950 *m*/*z* to 2000 *m*/*z*. The temperature of the ion transportation capillary was set at 350 °C. The mass resolution was 70,000. Maximum inject time, automatic gain control (AGC) target, sheath gas flow rate, aux gas flow rate, sweep gas flow rate and spray voltage were 100 ms, 5 × 10^5, 35 unit, 15 unit, 2 unit, and 3.20 kV, respectively.

2.5. The extract of the total RNA sample from cells

The human lung adenocarcinoma cell lines (A549) were incubated in complete medium (Dulbecco's Modified Eagle's Medium, supplemented with 10% fetal bovine serum (FBS) and 1% penicillin and streptomycin) at 37 °C in the atmosphere containing 5% CO_2. Incubated A549 cells were collected by trypsinization and centrifugation, washed with PBS, and pelleted at 3000 rpm for 5 min at 4 °C. The pellet was dissolved in 1 mL of TRIzol Reagent and 0.5 mL of isopropanol and incubated for 10 min. The mixture was centrifuged at 12,000×*g* for 10 min at 4 °C, then the supernatant was

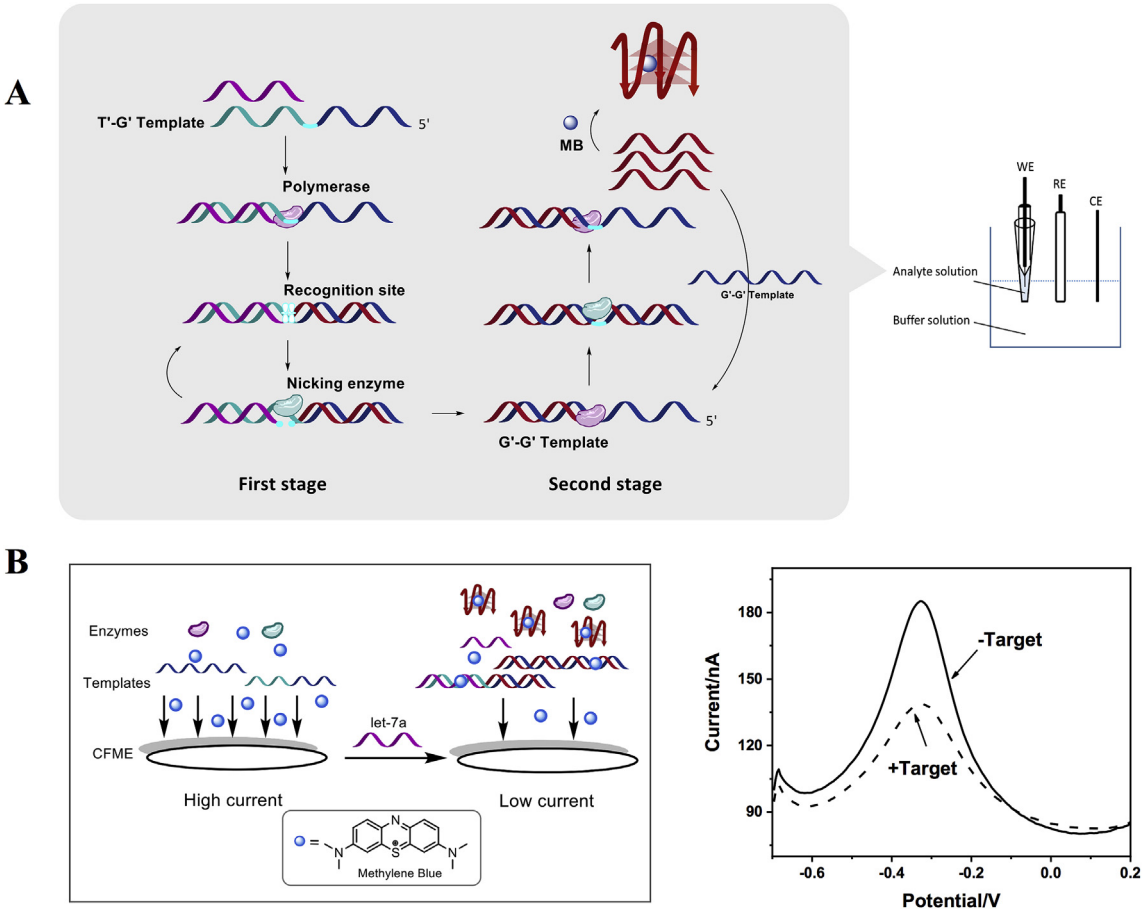

Scheme 1. The strategy of G3-EXPAR for miRNA detection. (A) Schematic representation of G3-EXPAR system. (B) Electrochemical readout based on G3/MB probe.

discarded with a micropipette. Subsequently, the pellet was resuspended in 1 mL of 75% ethanol and 1 mL of TRIzol Reagent then centrifuged for 5 min at 7500×*g* at 4 °C. Finally, the RNA pellet was air dried for 5–10 min after the supernatant was discarded. For miRNA detection, the pellet was resuspended in 50 μL of RNase-free water, 0.1 mM EDTA and 1 U/μL recombinant RNase Inhibitor. The RNA was highly pure as measured by Nanodrop (A_{260}/A_{280} = 2.0). The quantification was carried out by following the same procedure as described above, then the concentration of target miRNA was calculated.

3. Results and discussion

3.1. Principle of G3-EXPAR for miRNA detection

The strategy of G3-EXPAR is illustrated in Scheme 1A. The newly discovered G-triplex sequence (G3) could strongly bind with MB to cause a significant current decrease of MB [27]. Thus, G3 was chosen to conduct an electrochemical probe with MB in this work (Scheme 1B). G3-EXPAR contains two stages, linear amplification which enables the conversion of target miRNA to the reporter G3, and exponential amplification of G3 (Scheme 1A). In the first stage, the template (T′-G′) contains two different regions that are complementary to target miRNA and reporter G3, respectively, which are separated by a short NEase recognition sequence. Once the target miRNA hybridizes with the template, it is extended along with the template by Vent (exo-) DNA polymerase with strand displacement activity. The dsDNA containing the nicking recognition sequence is synthesized then cleaved by endonuclease Nt. BstNBI, thereby generating a nick. The polymerase can extend the 3′ end of the nicked site, which simultaneously displaces the newly synthesized strand G3. Through a polymerization, nicking, and displacement reaction cycle, miRNA is converted into G3 in linear amplification manner. Meanwhile, the exponential amplification reaction in the second stage is initiated by the hybridization of the created G3 and the template (G′-G′) which contains two repeated complementary sequences of G3. Then trace amounts of the G3 generated by the linear amplification could be exponentially amplified after the second-stage reaction. After amplification, MB was added into the amplification product to form a stable G3/MB complex. A 20 μL analyte solution was measured in the miniaturized electrochemical device with CFME as a working electrode. As shown in Scheme 1B, the forming G3/MB probe indicates the variation of current, which is used as a metric to determine the concentration of miRNA.

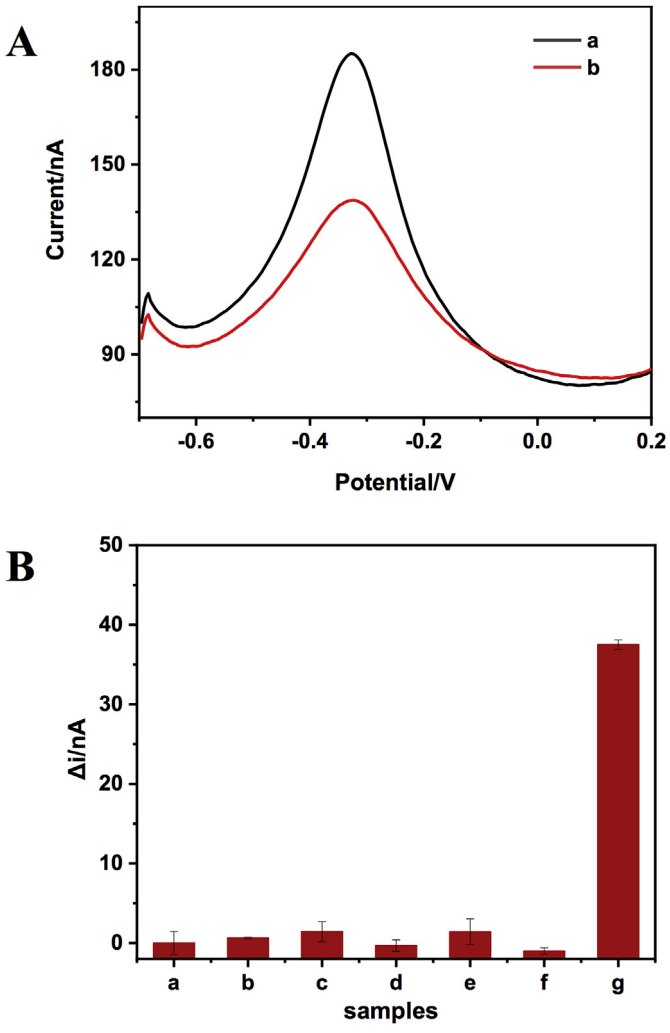

Fig. 1. (A) The SWV curves of (a) negative control, (b) G3-EXPAR production triggered by 1 nM let-7a. (B) The control experiments of G3-EXPAR: (a) two templates + two enzymes + dNTPs, (b) let-7a + T′-G′ template + two enzymes + dNTPs, (c) let-7a + G′-G′ template + two enzymes + dNTPs, (d) let-7a + two templates + Nt. BstNBI + dNTPs, (e) let-7a + two templates + Vent (exo-) polymerase + dNTPs, (f) let-7a + two templates + two enzymes, (g) let-7a + two templates + two enzymes + dNTPs.

3.2. Feasibility of G3-EXPAR

First, we validated the feasibility of the G3/MB complex as a signal generator by measuring the sensitivity of G3 detection according to the electrochemical response of MB. As shown in Figure S1, the diffusion current of MB was related to the concentration of G3. The higher the concentration of G3 was, the lower the current of MB was obtained. The lowest detectable concentration of G3 was 10 nM. Therefore, to meet the demand for sensitively detecting trace amounts of miRNA in the real sample, the efficient conversion of miRNA to G3 and a proper amplification of G3 should be introduced, which came out the strategy of G3-EXPAR shown in Scheme 1.

Using let-7a, a 22 nt miRNA as a model, we measured the SWVs of the amplification production triggered by 1 nM let-7a and without triggering (the negative control) using G3/MB as a signal generator. As depicted in Fig. 1A, the G3-EXPAR production

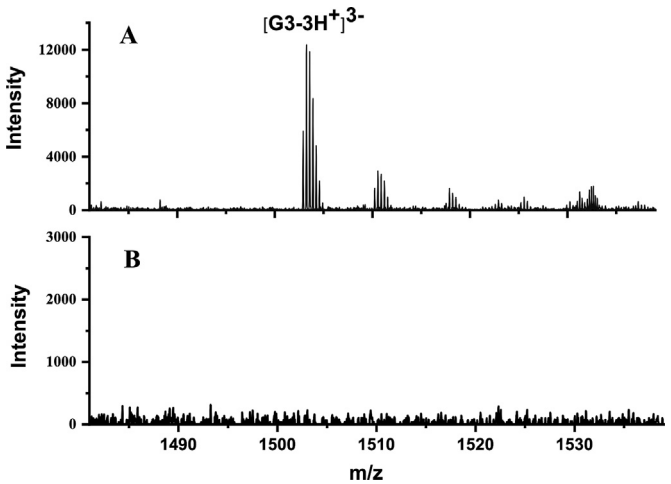

Fig. 2. Mass spectra of (A) G3-EXPAR production triggered by 1 nM target and (B) negative control.

triggered by 1 nM let-7a (curve b) shows a significant decrease in peak current compared with the negative control (curve a). It indicated that the G3-EXPAR strategy realized both the conversion of let-7a to the G3 sequence and the generation of a large amount of G3. The generated G3 was successfully detected via G3/MB system based on our miniaturized electrochemical device. For the proof-of-concept experiment, we carried out a series of experiments differing in reaction conditions. The EXPAR process involved two templates (T′-G′ and G′-G′), two enzymes (polymerase and nickase), and dNTPs. As shown in Fig. 1B, when five constituents (T′-G′ template, G′-G′ template, Vent (exo-) DNA polymerase, Nt. BstNBI nicking endonuclease, and dNTPs) co-existed in the EXPAR system, 1 nM let-7a could lead to a sharp decrease in SWV peak current (sample g) in comparison with the peak current generated by the negative control (sample a). However, when anyone among five constituents was absent, as seen from curve b, c, d, e, and f in Fig. 1B, no obvious peak current decrease was observed after the addition of 1 nM let-7a. The experiment results without dNTPs or polymerase or template indicated that the initiation of this amplification reaction was strictly dependent on all five constituents and target.

To prove the current decrease was caused by the large amount of G3 generated by EXPAR, LC-ESI-MS was performed. The MS spectra of the G3-EXPAR production triggered by 1 nM let-7a and the negative control are shown in Fig. 2A and B, respectively. It was seen in Fig. 2A that the G3 sequence [m/z 1503.24054 (−3)] could be easily identified. While from Fig. 2B, no obvious peaks for the reaction products were detected. Taken together, the results confirmed that the EXPAR assay was successfully carried out as designed in Scheme 1A.

3.3. The validation of the necessity of using the G3-EXPAR strategy

To verify the necessity of using the two-stage EXPAR assay, we compared its performance with that of T′-G′ strategy (Scheme 2A), which only included linear amplification of let-7a to G3. As shown by black columns in Fig. 3, the G3-EXPAR strategy could easily distinguish the concentrations of let-7a as low as 1 fM. However, the current obtained by T′-G′ strategy (blue columns) had no obvious change when the concentration of target let-7a was as high as 100 pM. We speculated that this might be because that the amplification efficiency of one-stage T′-G′ strategy was too low to produce enough amount of G3 to reach the detection limit of G3 by MB, which revealed the necessity of using the second-stage

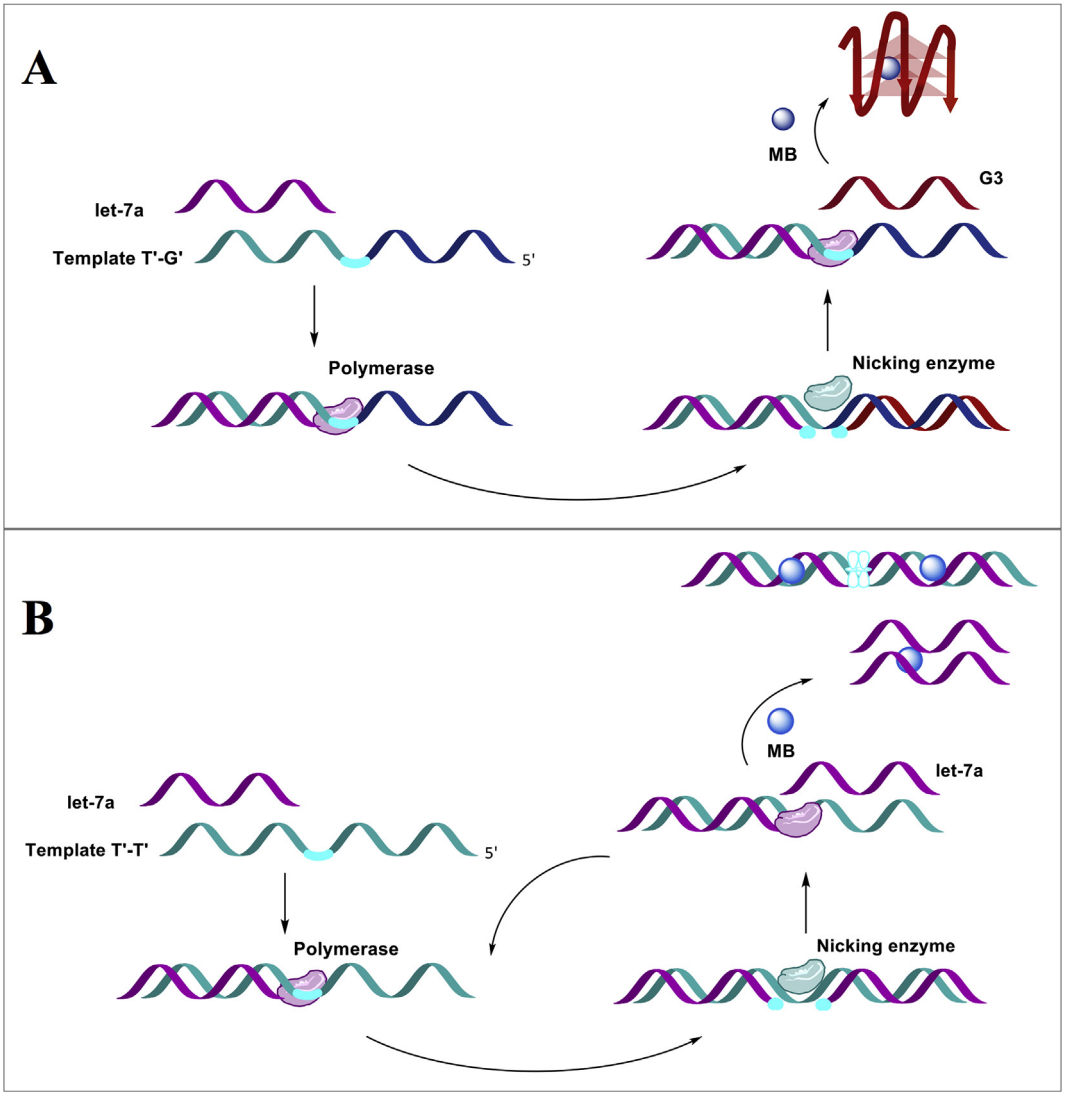

Scheme 2. (A) T′-G′ strategy for let-7a detection and (B) T′-T′ strategy for let-7a detection.

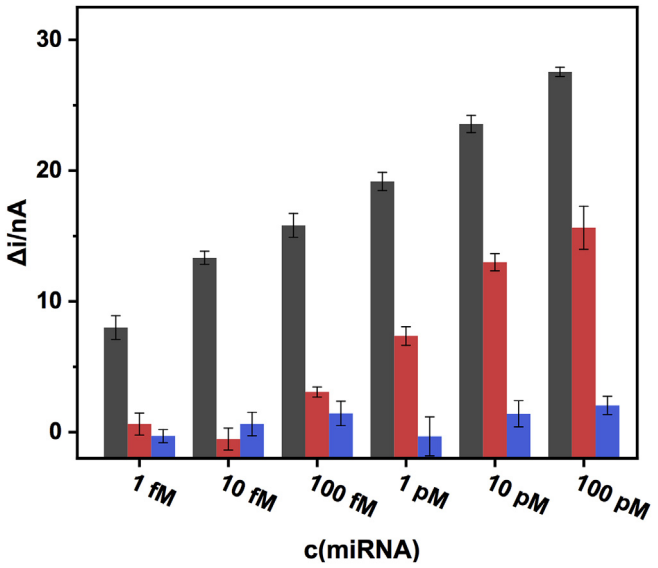

Fig. 3. Variation of the SWV peak currents ($\Delta i = i_{control} - i_{sample}$) in response to different concentrations of target let-7a (1 fM, 10 fM, 100 fM, 1 pM, 10 pM, and 100 pM) obtained by G3-EXPAR (black), T′-G′ (blue), and T′-T′ strategy (red). (For interpretation of the references to color in this figure legend, the reader is referred to the Web version of this article.)

exponential amplification of G3 through G′-G′ template. On the other hand, since MB could also non-specifically interact with ssDNA and dsDNA, the necessity of using G3/MB as a signal output was tested through comparing G3-EXPAR with that of T′-T′ strategy which represented only exponential amplification of target, let-7a (Scheme 2B). According to red columns (Fig. 3) obtained by T′-T′ strategy, the amplification production triggered by 100 fM let-7a only caused 3 nA current change to system. 10 fM or lower than 10 fM let-7a could not be distinguished between each other. Since the products produced by T′-T′ strategy were dsDNA formed by templates and a large amount of let-7a generated by the amplification, the result indicated that the products had a much weaker interaction with MB than G3 produced by G3-EXPAR, leading to the relatively lower sensitivity of T′-T′ strategy for miRNA. Generally, the above results indicated that G3-EXPAR strategy guaranteed the sensitive detection of let-7a.

3.4. Performance of G3-EXPAR for miRNA detection

We employed G3-EXPAR to detect different concentrations of target let-7a. It was observed in Fig. 4A that the SWV peak currents decreased along with the increase of the concentration of target let-7a. In the logarithmic scales, the variation of the SWV peak currents Δi ($\Delta i = i_{control} - i_{sample}$) exhibited a linear correlation with the concentration of target let-7a over a range of 7 orders of magnitude from 1 fM to 10 nM (Fig. 4B). The lowest detectable concentration was as low as 1 fM and the limit of detection was calculated to be 0.45 fM by evaluating the average signal of blank plus three times the standard deviation. Notably, the sensitivity of the proposed method is better than most of the assays for miRNA detection reported in recent years (Table S2) [32–40]. The improved sensitivity may be attributed to the highly efficient amplification of EXPAR with short G3 sequence and G3/MB as an electrochemical reporter.

An enormous challenge for miRNA analysis is the ability to distinguish between miRNA family members of small size and with high sequence homology. To investigate the specificity of the proposed method, four similar and relevant let-7 family miRNAs, let-7e, let-7f, let-7c, and let-7g, were tested using the same reaction

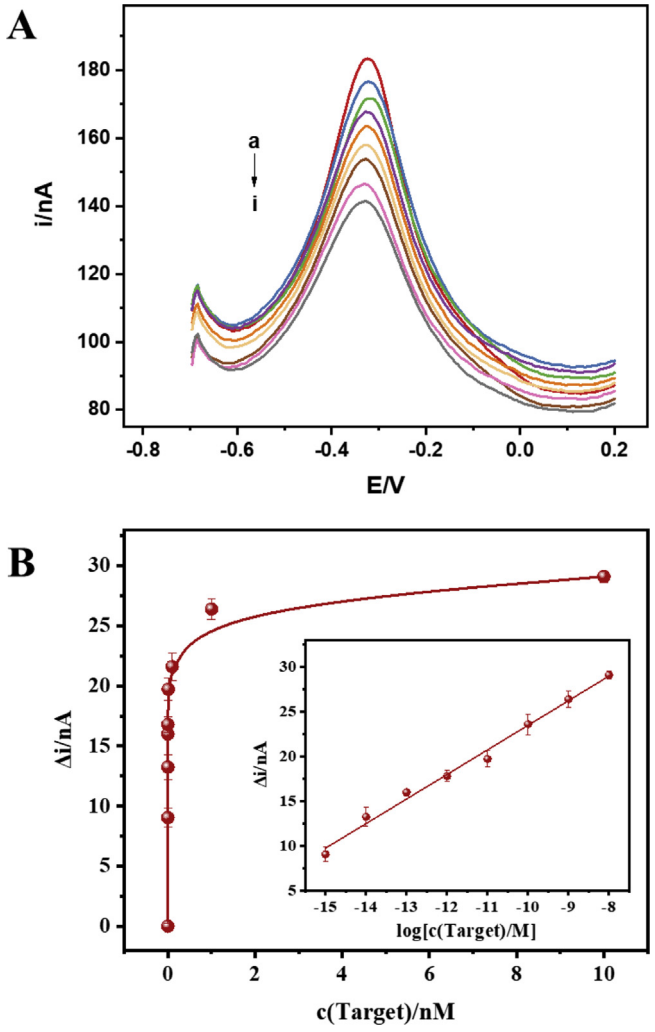

Fig. 4. (A) SWVs in response to different concentrations of target let-7a: (a) 0 fM, (b) 1 fM, (c) 10 fM, (d) 100 fM, (e) 1 pM, (f) 10 pM, (g) 100 pM, (h) 1 nM, (i) 10 nM. (B) Variations of the peak current Δi ($\Delta i = i_{control} - i_{sample}$) as a function of the target miRNA concentration. Inset: the linear relationship of currents versus the logarithm of target concentration in the range from 1 fM to 10 nM. Error bars showed the standard deviation of three experiments.

protocol described above. In detail, let-7e, let-7f, and let-7c contain one mismatch each and let-7g contains two mismatches. As shown in Fig. 5, the SWV peak current of let-7a was much lower than those of other miRNAs. The sensor exhibited good selectivity to let-7a as let-7a was the specific key to the initiation of the EXPAR reaction. The results indicated that the G3-EXPAR strategy had a good selectivity to target miRNA over the relevant let-7 family miRNAs.

In addition, the quantification performance of our system for a practical sample was evaluated. We evaluated the feasibility of monitoring the expression levels of miRNAs in the human lung adenocarcinoma cell lines (A549). The amount of let-7a miRNA in the total RNA sample of A549 cells was detected with the proposed miRNA assay by extract of the total RNA sample. To avoid the effect of the interferences from cell-derived RNA samples, the standard addition method was used. By adding known amounts of let-7a (10, 50, 100, and 500 zmol) standards to the practical sample, the amount of let-7a in the total RNA sample (1 ng) was estimated to be 179 zmol according to the obtained calibration curve (Figure S2). 1 ng of the total RNA samples spiked with let-7a at a final concentration of 10, 50 or 100 zmol showed a spiked recovery from 86%

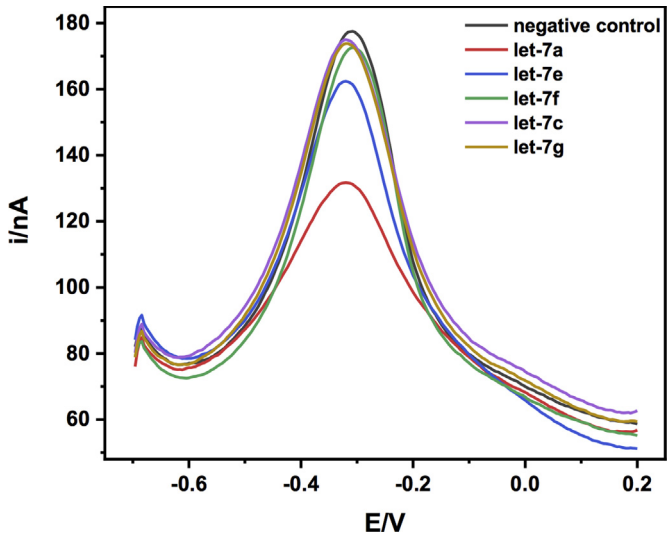

Fig. 5. SWVs of G3-EXPAR assay driven by 100 pM let-7a, let-7e, let-7f, let-7c, and let-7g, respectively.

to 117% and repeatability from 6.7% to 15% (Table S3). Therefore, the proposed method can be used to quantitatively detect as little as a zeptomole amount of miRNA in a total RNA sample with good accuracy and reproducibility. These results suggested that our proposed assay held great promise for sensitive quantification of miRNA in practical cell samples.

4. Conclusions

In summary, we developed a label-free, immobilization-free electrochemical biosensing platform for ultrasensitive detection of miRNA via G3-EXPAR. In this strategy, we converted miRNA to G3 and then amplified G3 exponentially to achieve an excellent detection sensitivity of the target miRNA based on the distinct current changes resulting from the high binding affinity between G3 and MB. By combining such a strategy with microliter electrochemical devices, we have made the detection of miRNAs simple, rapid, affordable, and convenient. We believe this simple, efficient, and sensitive signal read-out-mode based on G3/MB complex combining with EXPAR can be applied in the determination of different kinds of targets which are well-designed to generate G3 sequence, and our study can greatly facilitate the development of more functional and simpler homogeneous biosensing systems to support point-of-care detection and clinical diagnosis.

Declaration of competing interest

The authors declare that they have no known competing financial interests or personal relationships that could have appeared to influence the work reported in this paper.

CRediT authorship contribution statement

Ling-Li Zhao: Conceptualization, Methodology, Software, Investigation, Writing - original draft. **Hui-Yu Pan:** Validation, Formal analysis. **Xin-Xiang Zhang:** Resources, Visualization, Funding acquisition. **Ying-Lin Zhou:** Writing - review & editing, Project administration, Funding acquisition.

Acknowledgements

This work was supported by the National Natural Science Foundation of China (No. 21675004, 21575005 and 21775006).

Appendix A. Supplementary data

Supplementary data to this article can be found online at https://doi.org/10.1016/j.aca.2020.04.037.

References

[1] H. Dong, J. Lei, L. Ding, Y. Wen, H. Ju, X. Zhang, MicroRNA: function, detection, and bioanalysis, Chem. Rev. 113 (2013) 6207–6233.
[2] C.L. Sawyers, The cancer biomarker problem, Nature 452 (2008) 548–552.
[3] J. Lu, G. Getz, E.A. Miska, E. Alvarez-Saavedra, J. Lamb, D. Peck, A. Sweet-Cordero, B.L. Ebert, R.H. Mak, A.A. Ferrando, MicroRNA expression profiles classify human cancers, Nature 435 (2005) 834–838.
[4] N. Yanaihara, N. Caplen, E. Bowman, M. Seike, K. Kumamoto, M. Yi, R.M. Stephens, A. Okamoto, J. Yokota, T. Tanaka, Unique microRNA molecular profiles in lung cancer diagnosis and prognosis, Canc. Cell 9 (2006) 189–198.
[5] M. Lagos-Quintana, R. Rauhut, W. Lendeckel, T. Tuschl, Identification of novel genes coding for small expressed RNAs, Science 294 (2001) 853–858.
[6] P.T. Nelson, D.A. Baldwin, L.M. Scearce, J.C. Oberholtzer, J.W. Tobias, Z. Mourelatos, Microarray-based, high-throughput gene expression profiling of microRNAs, Nat. Methods 1 (2004) 155–161.
[7] A. Válóczi, C. Hornyik, N. Varga, J. Burgyán, S. Kauppinen, Z. Havelda, Sensitive and specific detection of microRNAs by northern blot analysis using LNA-modified oligonucleotide probes, Nucleic Acids Res. 32 (2004) e175-e175.
[8] E. Varkonyi-Gasic, R. Wu, M. Wood, E.F. Walton, R.P. Hellens, Protocol: a highly sensitive RT-PCR method for detection and quantification of microRNAs, Plant Methods 3 (2007) 12.
[9] Y. Zhou, Q. Huang, J. Gao, J. Lu, X. Shen, C. Fan, A dumbbell probe-mediated rolling circle amplification strategy for highly sensitive microRNA detection, Nucleic Acids Res. 38 (2010) e156-e156.
[10] J. Ge, Z. Qi, L. Zhang, X. Shen, Y. Shen, W. Wang, Z. Li, Label-free and enzyme-free detection of microRNA based on a hybridization chain reaction with hemin/G-quadruplex enzymatic catalysis-induced MoS 2 quantum dots via the inner filter effect, Nanoscale 12 (2020) 808–814.
[11] C. He, M. Wang, X. Sun, Y. Zhu, X. Zhou, S. Xiao, Q. Zhang, F. Liu, Y. Yu, H. Liang, Integrating PDA microtube waveguide system with heterogeneous CHA amplification strategy towards superior sensitive detection of miRNA, Biosens. Bioelectron. 129 (2019) 50–57.
[12] H.-X. Jiang, Z.-Z. Liang, Y.-H. Ma, D.-M. Kong, Z.-Y. Hong, G-quadruplex fluorescent probe-mediated real-time rolling circle amplification strategy for highly sensitive microRNA detection, Anal. Chim. Acta 943 (2016) 114–122.
[13] D.W. Wegman, S.N. Krylov, Direct quantitative analysis of multiple miRNAs (DQAMmiR), Angew. Chem. Int. Ed. 50 (2011) 10335–10339.
[14] L. Ge, W. Wang, F. Li, Electro-grafted electrode with graphene-oxide-like DNA affinity for ratiometric homogeneous electrochemical biosensing of microRNA, Anal. Chem. 89 (2017) 11560–11567.
[15] T. Hou, N. Xu, W. Wang, L. Ge, F. Li, Truly immobilization-free diffusivity-mediated photoelectrochemical biosensing strategy for facile and highly sensitive microRNA assay, Anal. Chem. 90 (2018) 9591–9597.
[16] T.G. Drummond, M.G. Hill, J.K. Barton, Electrochemical DNA sensors, Nat. Biotechnol. 21 (2003) 1192–1199.
[17] X. Bo, M. Zhou, L. Guo, Electrochemical sensors and biosensors based on less aggregated graphene, Biosens. Bioelectron. 89 (2017) 167–186.
[18] H.-A. Rafiee-Pour, M. Behpour, M. Keshavarz, A novel label-free electrochemical miRNA biosensor using methylene blue as redox indicator: application to breast cancer biomarker miRNA-21, Biosens. Bioelectron. 77 (2016) 202–207.
[19] C. Pöhlmann, M. Sprinzl, Electrochemical detection of microRNAs via gap hybridization assay, Anal. Chem. 82 (2010) 4434–4440.
[20] M. Azimzadeh, M. Rahaie, N. Nasirizadeh, K. Ashtari, H. Naderi-Manesh, An electrochemical nanobiosensor for plasma miRNA-155, based on graphene oxide and gold nanorod, for early detection of breast cancer, Biosens. Bioelectron. 77 (2016) 99–106.
[21] E. Lusi, M. Passamano, P. Guarascio, A. Scarpa, L. Schiavo, Innovative electrochemical approach for an early detection of microRNAs, Anal. Chem. 81 (2009) 2819–2822.
[22] Z. Fredj, S. Azzouzi, A.P. Turner, M.B. Ali, W.C. Mak, Neutravidin biosensor for direct capture of dual-functional biotin-molecular beacon-AuNP probe for sensitive voltammetric detection of microRNA, Sensor. Actuator. B Chem. 248 (2017) 77–84.
[23] S. Azzouzi, Z. Fredj, A.P. Turner, M.B. Ali, W.C. Mak, Generic neutravidin biosensor for simultaneous multiplex detection of microRNAs via electrochemically encoded responsive nanolabels, ACS Sens. 4 (2019) 326–334.
[24] P. Gai, C. Gu, H. Li, X. Sun, F. Li, Ultrasensitive ratiometric homogeneous electrochemical microRNA biosensing via target-triggered Ru (III) release and redox recycling, Anal. Chem. 89 (2017) 12293–12298.

[25] J. Chang, X. Wang, J. Wang, H. Li, F. Li, Nucleic acid-functionalized metal–organic framework-based homogeneous electrochemical biosensor for simultaneous detection of multiple tumor biomarkers, Anal. Chem. 91 (2019) 3604–3610.
[26] P. Gai, C. Gu, T. Hou, F. Li, Integration of biofuel cell-based self-powered biosensing and homogeneous electrochemical strategy for ultrasensitive and easy-to-use bioassays of MicroRNA, ACS Appl. Mater. Interfaces 10 (2018) 9325–9331.
[27] L.-L. Zhao, T. Cao, Q.-Y. Zhou, X.-H. Zhang, Y.-L. Zhou, L. Yang, X.-X. Zhang, The exploration of a New stable G-triplex DNA and its novel function in electrochemical biosensing, Anal. Chem. 91 (2019) 10731–10737.
[28] H. Jia, Z. Li, C. Liu, Y. Cheng, Ultrasensitive detection of microRNAs by exponential isothermal amplification, Angew. Chem. Int. Ed. 49 (2010) 5498–5501.
[29] Y.-P. Zhang, Y.-X. Cui, X.-Y. Li, Y.-C. Du, A.-N. Tang, D.-M. Kong, A modified exponential amplification reaction (EXPAR) with an improved signal-to-noise ratio for ultrasensitive detection of polynucleotide kinase, Chem. Commun. 55 (2019) 7611–7614.
[30] X. Li, Y. Cui, Y. Du, A. Tang, D. Kong, Label-free telomerase detection in single cell using a five-base telomerase product-triggered exponential rolling circle amplification strategy, ACS Sens. 4 (2019) 1090–1096.
[31] D.-W. Zhang, J.-X. Liu, J. Nie, Y.-L. Zhou, X.-X. Zhang, Micropipet tip-based miniaturized electrochemical device combined with ultramicroelectrode and its application in immobilization-free enzyme biosensor, Anal. Chem. 85 (2013) 2032–2036.
[32] T. Hou, W. Li, X. Liu, F. Li, Label-free and enzyme-free homogeneous electrochemical biosensing strategy based on hybridization chain reaction: a facile, sensitive, and highly specific microRNA assay, Anal. Chem. 87 (2015) 11368–11374.
[33] Y. Zhou, H. Yin, J. Li, B. Li, X. Li, S. Ai, X. Zhang, Electrochemical biosensor for microRNA detection based on poly (U) polymerase mediated isothermal signal amplification, Biosens. Bioelectron. 79 (2016) 79–85.
[34] R. Wang, L. Wang, H. Zhao, W. Jiang, A split recognition mode combined with cascade signal amplification strategy for highly specific, sensitive detection of microRNA, Biosens. Bioelectron. 86 (2016) 834–839.
[35] Q. Liu, P.-J. Kang, Z. Chen, C.-X. Shi, Y. Chen, R. Yu, Highly specific and sensitive detection of microRNAs by tandem signal amplification based on duplex-specific nuclease and strand displacement, Chem. Commun. 55 (2019) 14210–14213.
[36] Z. Zhang, Y. Wang, N. Zhang, S. Zhang, Self-assembly of nucleic acid molecular aggregates catalyzed by a triple-helix probe for miRNA detection and single cell imaging, Chem. Sci. 7 (2016) 4184–4189.
[37] J. Dong, G. Chen, W. Wang, X. Huang, H. Peng, Q. Pu, F. Du, X. Cui, Y. Deng, Z. Tang, Colorimetric PCR-based microRNA detection method based on small organic dye and single enzyme, Anal. Chem. 90 (2018) 7107–7111.
[38] F. Xu, T. Yang, Y. Chen, Quantification of microRNA by DNA–Peptide probe and liquid chromatography–tandem mass spectrometry-based quasi-targeted proteomics, Anal. Chem. 88 (2015) 754–763.
[39] J. Li, P. Lei, S. Ding, Y. Zhang, J. Yang, Q. Cheng, Y. Yan, An enzyme-free surface plasmon resonance biosensor for real-time detecting microRNA based on allosteric effect of mismatched catalytic hairpin assembly, Biosens. Bioelectron. 77 (2016) 435–441.
[40] W. Lu, Y. Chen, Z. Liu, W. Tang, Q. Feng, J. Sun, X. Jiang, Quantitative detection of microRNA in one step via next generation magnetic relaxation switch sensing, ACS Nano 10 (2016) 6685–6692.